It is clear that much work needs to be done to address the relationship between solvent-induced conformation and reactivity of SAM functionalities.

The free energy of cell adhesion on solid surfaces is determined by the interfacial tensions between the cell, substrate, and liquid media.[36] EDA is suitable for the patterned adhesion of at least five types of cells (this report and refs 2 and 4), suggesting that it is the overall electrostatic and thermodynamic properties of the EDA and 13F surfaces that determine the adhesion, rather than a type of specific recognition between molecules on the substrate and cell surfaces. In this case, EDA (and unirradiated EDA exposed to 13F) provided suitable growth substrates for two types of explanted mammalian cells for which the standard growth substrates are loosely-packed polymers (polylysine, collagen). This suggests that the apparent disorder of EDA films might actually be *advantageous* for cell adhesion. The minor reaction of 13F with EDA-treated surfaces did not have a noticeable affect on cell adhesion. This is not surprising, since the equilibrium values of θ_a were nearly the same for pure EDA and for EDA treated with 13F in toluene or chloroform. It should be pointed out that proposed mechanisms of cell adhesion to SAMs must first account for the amount and nature of protein constituents of the cell culture media that bind to the substrate prior to the cells.[37,38]

Recent reports[39] indicate that silane-coupled cell adhesion peptide fragments can be used to affect the adhesion and growth of specific types of cells through molecular recognition. Future experiments may optimize the use of deep UV-defined patterns as templates for covalent attachment of these and other families of cell adhesion molecules[40] that may be used to further direct cell morphology and function.

Acknowledgment. This work was supported in part by the Office of Naval Research and the Office of Naval Technology (DAS), the Naval Medical Research Development Command (TBN; work unit No. MR04120.001-1002), and the MANTECH office of the Assistant Secretary of the Navy (J.M.C.). We acknowledge Steve McElvany for assistance with FTMS experiments and Tim Koloski (ONT Post-Doctoral Fellow) for NMR experiments. We thank Dr. Forrest Weight (National Institute of Alcohol Abuse and Alcoholism) for the generous use of animal care and cell culture facilities and Drs. Kenneth and Wendy Scholz (University of Chicago), and Gary Banker (University of Virginia) for advice and helpful conversations concerning neuron culture. We acknowledge the reviewers of this manuscript, whose careful attention to detail and constructive criticisms are greatly appreciated. The opinions and assertions contained herein are the private ones of the authors and are not to be construed as official or reflecting the views of the Navy Department or the naval service at large.

Registry No. EDA, 1760-24-3; 13F, 102488-47-1; silica, 7631-86-9.

(36) Dicosmo, F.; Facchini, P. J.; Neumann, A. W. *Colloids and Surfaces* **1989**, *42*, 255.
(37) Prime, K. L.; Whitesides, G. M. *Science* **1991**, *252*, 1164-1167.
(38) Lee, S. H.; Ruckenstein, E. *J. Colloid Interface Sci.* **1988**, *125*, 365-379.
(39) Massia, S. P.; Hubbell, J. A. *Anal. Biochem.* **1990**, *187*, 292-301.
(40) Albelda, S. M.; Buck, C. A. *FASEB J.* **1990**, *4*, 2868-2880.

Deuterium Isotope Effects in Constrained Tryptophan Derivatives: Implications for Tryptophan Photophysics

Lloyd P. McMahon, William J. Colucci,† Mark L. McLaughlin,* and Mary D. Barkley*

Contribution from the Department of Chemistry, Louisiana State University, Baton Rouge, Louisiana 70803-1804. *Received January 14, 1992*

Abstract: The deuterium isotope effect on the fluorescence quantum yield and lifetime of the constrained tryptophan derivative 3-carboxy-1,2,3,4-tetrahydro-2-carboline, W(1), was determined as a function of pH and temperature. The isotope effect between pH 3.5 and 11 is attributed to a temperature-dependent quenching process common to all indoles. At room temperature the quantum yield ratio in D_2O and H_2O is 1.05 for W(1) zwitterion and 1.7 for W(1) anion. The temperature dependence of the fluorescence lifetime was determined for the zwitterion and the anion in H_2O and D_2O. The frequency factors A and activation energies E^* in H_2O are $A = 6 \times 10^{16}$ s^{-1}, $E^* = 12.6$ kcal/mol for W(1) zwitterion and $A = 5 \times 10^{16}$ s^{-1}, $E^* = 11.8$ kcal/mol for W(1) anion, compared to $A = 8 \times 10^{16}$ s^{-1}, $E^* = 13.1$ kcal/mol for *N*-methylindole. The radiative rates, temperature-independent nonradiative rates, and activation energies E^* of W(1) zwitterion, W(1) anion, and *N*-methylindole are insensitive to solvent isotope. The frequency factors A of these compounds are 2- to 3-fold larger in H_2O than in D_2O. The large deuterium isotope effect in W(1) anion at room temperature compared to W(1) zwitterion results from two factors: a smaller temperature-independent nonradiative rate and a larger isotopically sensitive temperature-dependent rate. Several mechanisms for the intrinsic deuterium isotope effect are discussed. Two mechanisms are consistent with available data for indoles: "invisible" or incomplete proton transfer from water to indole and formation of a water–indole charge-transfer exciplex.

Tryptophan, W, has been much studied because of its importance as an intrinsic fluorescent probe of conformation and dynamics in proteins. The complex photophysics, however, make interpretation of fluorescence results difficult.[1] Multiexponential fluorescence decays appear to be the rule, rather than the exception, for tryptophan derivatives as well as for proteins containing a single tryptophan.[2] In some proteins the fluorescence decay of the single tryptophan approaches a continuous distribution of lifetimes.[3] One explanation for the lifetime heterogeneity invokes multiple ground-state conformers or microconformational states that do not interconvert on the fluorescence time scale. In the conformer model, the lifetime differences among conformers are attributed to differences in proximity of functional groups that

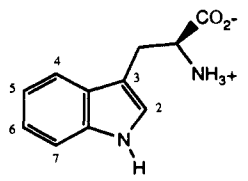

W

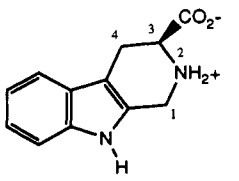

W(1)

† Present address: Ethyl Corp., Ethyl Technical Center, 8000 GSRI Ave., Baton Rouge, LA 70820.

(1) Creed, D. *Photochem. Photobiol.* **1984**, *39*, 537-562.
(2) Beechem, J. M.; Brand, L. *Annu. Rev. Biochem.* **1985**, *54*, 43-71.
(3) Alcala, J. R.; Gratton, E.; Prendergast, F. G. *Biophys. J.* **1987**, *51*, 925-936.

0002-7863/92/1514-8442$03.00/0

quench indole fluorescence.[4-7] For the most part, though, it has been impossible to assign lifetimes to conformers or to establish quenching mechanisms.

Recently, we obtained direct evidence for the conformer model using a rotationally constrained tryptophan derivative, 3-carboxy-1,2,3,4-tetrahydro-2-carboline, W(1). W(1) has a closely spaced biexponential decay.[8,9] Conformational analyses by X-ray crystallography, MM2, and NMR showed that W(1) adopts two stable conformations in solution differing in distance between the carboxylate and the indole ring. The conformer populations produced by MM2 and NMR correlated with the relative amplitudes of the biexponential decay well enough to assign the two lifetimes to the two ground-state conformers. The shorter lifetime is associated with the conformer having the carboxylate closest to the indole ring. In addition to reducing the number of rotational degrees of freedom, the stereochemical constraint in W(1) prevents the intramolecular excited-state proton transfer reaction that quenches the fluorescence of the tryptophan zwitterion.[10] We therefore identified through-space intramolecular electron transfer from the excited indole to the carboxylate as the probable cause of the lifetime difference.

It has been known for three decades that the fluorescence quantum yields and lifetimes of tryptophan and other indoles have distinctive deuterium isotope effects.[11-15] Ring carbon-substituted methyl indoles exhibit quantum yield profiles that are independent of pH from roughly pH 3 to 11, falling off rapidly at lower and higher pH.[14,16] In the plateau region simple indoles have quantum yield ratios in D_2O and H_2O ranging from 1.3 for indole to 2.8 for 2,4,6-trimethylindole.[15] Tryptophan, in contrast, has a quantum yield profile that is pH dependent. The quantum yield is constant from pH 4 to 8.5 and rises until pH 11, above which it drops as do other indoles.[14,17-19] The unusual rise at alkaline pH follows the titration of the amino group on the alanyl side chain. The isotope effect at neutral pH in tryptophan and other indole derivatives having a protonated amino group has been attributed to intramolecular quenching by excited-state proton transfer.[13,14] The intramolecular process was subsequently demonstrated to be proton exchange in photochemical isotope exchange experiments monitored by NMR.[10,20,21] As the amino group is deprotonated this mechanism is shut down, with an accompanying increase in quantum yield. The deuterium isotope effect persists throughout the entire pH range, the quantum yield ratio in D_2O and H_2O being about 2 at neutral pH and 1.4 at alkaline pH.[14,15] When tryptophan is in a peptide with a blocked amino terminus, the quantum yield profile and deuterium isotope effect are similar to those of simple indoles.[14]

Deuterium isotope effects on fluorescence have been interpreted as evidence for excited-state proton transfer reactions.[11] In cases where proton transfer quenches the fluorescence, the slower rate of deuteron transfer compared to proton transfer increases the quantum yield and lifetime of the excited state. There being no obvious proton transfer reaction in simple indoles at intermediate pH, the intrinsic isotope effect has been ascribed variously to such processes as internal conversion,[14] tunneling to the ground state,[12] and photoionization.[13,22,23] In this paper, we determine the deuterium isotope effect on the fluorescence quantum yield and lifetime of the constrained tryptophan W(1) as a function of pH and temperature. The isotope effect is attributed to a temperature-dependent quenching process that occurs in all indoles. Possible mechanisms for the isotopically sensitive nonradiative process are proposed and discussed in light of other data in the literature.

Experimental Section

Chemicals. 3-Carboxy-1,2,3,4-tetrahydro-2-carboline (W(1)), 3-amino-3-carboxy-1,2,3,4-tetrahydrocarbazole (W(2)), and 3-carboxy-1,2,3,4-tetrahydrocarbazole (W(1c)) were synthesized as described elsewhere.[8,24,25] 1,2,3,4-Tetrahydrocarbazole, THC, and 1,2,3,4-tetrahydro-2-carboline, W(1a), were purchased from Aldrich and purified as described elsewhere.[24,25] *N*-Methylindole (Aldrich) was distilled before use. Compounds were dissolved in 0.01 M phosphate-buffered H_2O or D_2O (Sigma, 99.9 atom% D). pD was adjusted using DCl and NaOD. pH and pD were measured on a Beckman pHI 34 meter with a Beckman Model 39536 electrode. pD was calculated from the pH meter reading as pD = pH + 0.4.[26]

Absorbance. Absorbance was measured on an Aviv 118DS spectrophotometer in 1-cm cells. The pK was determined by measuring absorbance changes at 278 nm.[27] Sample absorbance was adjusted to <0.1 at 280 nm for steady-state fluorescence measurements and <0.2 at 296 nm for time-resolved measurements.

Fluorescence Quantum Yields. Quantum yields were determined by the reference method on an SLM 8000 spectrofluorometer interfaced to a Macintosh IIcx computer. Temperature was maintained at 25 °C with a Lauda circulating bath. Samples were excited at 280 nm. Spectra were collected in ratio mode with single excitation and emission monochromators set at 4- and 8-nm bandpass, respectively. Magic angle polarizers were set to 55° on the excitation side and 0° on the emission side to avoid the Wood's anomaly of the emission grating. A solvent blank was subtracted, and spectra were corrected for wavelength-dependent instrument response using correction factors determined with a standard lamp from Optronics. Quantum yields were measured relative to tryptophan (Sigma, recrystallized four times from 70% ethanol) in water using a value of 0.14 for tryptophan.[28]

Time-Resolved Fluorescence. Fluorescence lifetimes were measured by time-correlated single photon counting on a Photochemical Research Associates instrument with a picosecond dye laser excitation source. The synchronously pumped dye laser system consists of a Quantronix Model 416 Nd-YAG laser with modelocker, stabilizer, and frequency doubler and a Coherent Model 701-3 dye laser with cavity dumper. The modelocker temperature was maintained at 23 °C with a Neslab circulating bath to improve stability of the pump beam. The laser dye was rhodamine 6G (Exciton). The output beam from the dye laser was passed through a BBO crystal to frequency double into the UV, a half-wave retarder to rotate the polarization, a Newport 935 attenuator to adjust the intensity, and a Pellin-Broca crystal to remove the fundamental. The Ortec 457 time-to-amplitude converter was operated in reverse mode. The stop timing signal was provided by a portion of the dye laser output, which was detected by an Antel Optronics AR-S2 fast photodiode, amplified by a Tennelec 454 quad constant fraction discriminator, and delayed by a Tennelec 412A delay. The start timing signal was provided by the fluorescence emission, which was detected by a cooled Hamamatsu R955 photomultiplier, amplified by a PRA 1763 fast preamplifier, and discriminated by an Ortec 583 constant fraction discriminator. The R955 photomultiplier was run at 1380 V with 200 V applied across the first dynode, 6-nF capacitors between dynodes 6 through 8, and 0.1-μF ca-

(4) Donzel, B.; Gauduchon, P.; Wahl, Ph. *J. Am. Chem. Soc.* **1974**, *96*, 801-808.
(5) Szabo, A. G.; Rayner, D. M. *J. Am. Chem. Soc.* **1980**, *102*, 554-563.
(6) Petrich, J. W.; Chang, M. C.; McDonald, D. B.; Fleming, G. R. *J. Am. Chem. Soc.* **1983**, *105*, 3824-3832.
(7) Ross, J. B. A.; Wyssbrod, H. R.; Porter, R. A.; Schwartz, G. P.; Michaels, C. A.; Laws, W. R. *Biochemistry* **1992**, *31*, 1585-1594.
(8) Tilstra, L.; Sattler, M. C.; Cherry, W. R.; Barkley, M. D. *J. Am. Chem. Soc.* **1990**, *112*, 9176-9182.
(9) Colucci, W. J.; Tilstra, L.; Sattler, M. C.; Fronczek, F. R.; Barkley, M. D. *J. Am. Chem. Soc.* **1990**, *112*, 9182-9190.
(10) Saito, I.; Sugiyama, H.; Yamamoto, A.; Muramatsu, S.; Matsuura, T. *J. Am. Chem. Soc.* **1984**, *106*, 4286-4287.
(11) Stryer, L. *J. Am. Chem. Soc.* **1966**, *88*, 5708-5712.
(12) Eisinger, J.; Navon, G. *J. Chem. Phys.* **1969**, *50*, 2069-2077.
(13) Kirby, E. P.; Steiner, R. F. *J. Phys. Chem.* **1970**, *74*, 4480-4490.
(14) Lehrer, S. S. *J. Am. Chem. Soc.* **1970**, *92*, 3459-3462.
(15) Ricci, R. W. *Photochem. Photobiol.* **1970**, *12*, 67-75.
(16) Vander Donckt, E. *Bull. Soc. Chim. Belg.* **1969**, *78*, 69-75.
(17) White, A. *Biochem. J.* **1959**, *71*, 217-220.
(18) Cowgill, R. W. *Arch. Biochem. Biophys.* **1963**, *100*, 36-44.
(19) De Lauder, W. B.; Wahl, Ph. *Biochemistry* **1970**, *9*, 2750-2754.
(20) Shizuka, H.; Serizawa, M.; Kobayashi, H.; Kameta, K.; Suglyama, H.; Matsuura, T.; Saito, I. *J. Am. Chem. Soc.* **1988**, *110*, 1726-1732.
(21) Shizuka, H.; Serizawa, M.; Shimo, T.; Saito, I.; Matsuura, T. *J. Am. Chem. Soc.* **1988**, *110*, 1930-1934.
(22) Robbins, R. J.; Fleming, G. R.; Beddard, G. S.; Robinson, G. W.; Thistlethwaite, P. J.; Woolfe, G. J. *J. Am. Chem. Soc.* **1980**, *102*, 6271-6279.
(23) Lee, J.; Robinson, G. W. *J. Phys. Chem.* **1985**, *89*, 1872-1875.
(24) Yu, H.-T.; McMahon, L. P.; Vela, M. A.; McLaughlin, M. L.; Fronczek, F. R.; Barkley, M. D., in preparation.
(25) Yu, H.-T.; Vela, M. A.; McLaughlin, M. L.; Fronczek, F. R.; Barkley, M. D., in preparation.
(26) Lumry, R.; Smith, E. L.; Glantz, R. R. *J. Am. Chem. Soc.* **1951**, *73*, 4330-4340.
(27) Hermans, J., Jr.; Donovan, J. W.; Scheraga, H. A. *J. Biol. Chem.* **1960**, *235*, 91-93.
(28) Chen, R. F. *Anal. Lett.* **1967**, *1*, 35-42.

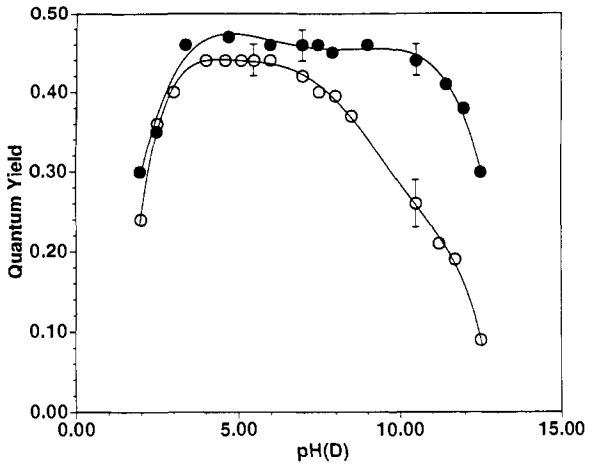

Figure 1. pH dependence of fluorescence quantum yield of W(1) in (○) H_2O and (●) D_2O at 25 °C.

pacitors between the last two dynodes and the anode. The width of the instrument response was 350–400 ps FWHM. An excitation wavelength of 296 nm was selected with a three-plate birefringent filter. The exciting light was vertically polarized; the emission polarizer was oriented at 55°. Emission wavelength was selected with an Instruments SA H-10 monochromator at 8-nm bandpass. The excitation rate was 760 kHz; emission rates were <8 kHz. Cell holder temperature was regulated with a Neslab circulating bath; cell temperature was monitored with an Omega thermistor.

Fluorescence decays for sample and reference fluorophore were acquired contemporaneously in 512 channels of 27.0, 54.0, or 108 ps/channel to about 2.5×10^4 counts in the peak. The instrument was controlled by a Macintosh IIcx computer running data acquisition software based on LabVIEW.[29] Solutions of *p*-terphenyl (Aldrich, 99+%) in ethanol or 75% ethanol, 0.8 M KI (containing a trace of thiosulfate to retard I_3^- formation) were used as reference fluorophores. Lifetimes of 1.06–1.12 ns for terphenyl and 0.18–0.20 ns for quenched terphenyl were determined in separate experiments using *N*-acetyltryptophanamide (Sigma) in water as the monoexponential standard. Decay data were fitted by reference deconvolution to a sum of exponentials with amplitudes α_i and lifetimes τ_i.[30] Decay curves acquired at different emission wavelengths were deconvolved using the Beechem global program with the lifetimes linked.[31] Decay curves acquired at different temperatures were analyzed in the Beechem program assuming monoexponential functions given by eq 6.

Results and Discussion

p*K*. Tryptophan derivatives exchange the indole nitrogen and amino protons for deuterium when dissolved in D_2O. Exchange of deuterons for protons causes slight increases in the p*K*s of various functional groups.[32] The pK_D of the amino group of W(1) was determined by absorbance to be about 9.5. A value of 9.41 was calculated from an empirical expression using p*K* shifts for α-amino groups.[32] In W(1) pK_D is 0.7 unit more basic than is the pK_H, 8.8.[8] The p*K* shift of the tryptophan amino group measured by fluorescence was also 0.7 unit.[14]

pH Dependence of Quantum Yield. The fluorescence quantum yield of W(1) was measured from pH(D) 2.0 to 12.5 in H_2O and D_2O. The quantum yield profiles at 25 °C are shown in Figure 1. The profile of W(1) in D_2O is typical of simple indoles. However, the profile in H_2O is different.[33] At the extremes of pH, the quantum yields in both H_2O and D_2O show the steep drops characteristic of indole derivatives. In the acidic region below about pH(D) 3, the quenching mechanism is generally considered to be acid-catalyzed ring protonation.[16,17,34] Likely protonation sites are C3 and N1 of the indole ring, which correspond to ground-state protonation sites of indoles in aqueous acids.[35] The p*K* for protonation of 2,3-dimethylindole in the ground state is −1.49.[36] The excited-state p*K** for protonation of W(1), a 2,3-dialkylindole, estimated from Figure 1 is about 1.9. This implies that W(1) becomes a stronger base in the excited state. Comparable increases (1.5–6.7 pH units) in basicity have been noted for simple indoles.[14,16] In the alkaline region above pH(D) 11, the fluorescence is quenched by deprotonation of the indole nitrogen.[16,37] *N*-Methylindole, which lacks the indole N–H proton, does not show a drop in fluorescence at high pH.[16] The ground-state p*K* for deprotonation of the indole nitrogen is 16–17.[38] The excited-state p*K** for deprotonation of W(1) is probably around 12 (Figure 1), which is similar to the values of 11.6–12.6 for simple indoles.[14,16] The indole N–H proton becomes more acidic in the excited state by 4–5 pH units.

Between pH(D) 3.5 and 11 is the area of real interest, where W(1) departs from the usual behavior of indole compounds. From

Table I. Fluorescence Quantum Yields in H_2O and D_2O at 25 °C

	Φ^a	$\bar{\tau}$,[b] ns	10^{-7} k_r, s^{-1}	10^{-7} k_{nr}, s^{-1}	ref
		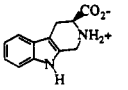			
		W(1)			
pH 5.5	0.44 ± 0.02	6.01	7.3 ± 0.3	9.3 ± 0.3	9
pD 7.0	0.46 ± 0.02	5.72	8.0 ± 0.3	9.4 ± 0.3	
pH 10.5	0.26 ± 0.03	4.40	5.9 ± 0.7	17 ± 1	9
pD 10.5	0.44 ± 0.02	7.44	5.9 ± 0.3	7.5 ± 0.3	
		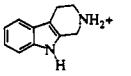			
		W(1a)			
pH 5.5	0.38 ± 0.02	5.61 ± 0.05	6.8 ± 0.4	11 ± 1	25
pD 5.5	0.42 ± 0.02	7.06 ± 0.04	6.0 ± 0.3	8.2 ± 0.3	25
pH 10.5	0.21	4.46	4.7	18	25
pD 10.5	0.31				25
		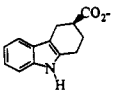			
		W(1c)			
pH 7.0	0.14 ± 0.02	3.63 ± 0.04	3.9 ± 0.5	24 ± 1	24
pD 7.0	0.27 ± 0.03	6.98 ± 0.06	3.9 ± 0.4	10 ± 1	24
					
		THC			
pH 7.0	0.12 ± 0.01	3.12 ± 0.06	3.9 ± 0.3	28 ± 1	24
pD 7.0	0.25 ± 0.02	6.41 ± 0.05	3.9 ± 0.3	12 ± 1	24
		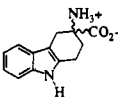			
		W(2)			
pH 6.0	0.35 ± 0.02	4.41	7.9 ± 0.5	15 ± 1	25
pD 6.0	0.52 ± 0.02	6.58	7.9 ± 0.3	7.3 ± 0.3	25
pH 11.0	0.21	3.75 ± 0.02	5.6	21	25
pD 11.0	0.37	7.36 ± 0.02	5.0	8.6	25

[a] 280-nm excitation wavelength. Errors from 2 to 5 experiments. [b] 296-nm excitation wavelength. Errors from 2 to 5 experiments.

(29) Stryjewski, W. *Rev. Sci. Instrum.* **1991**, *62*, 1921–1925.
(30) Kolber, Z. S.; Barkley, M. D. *Anal. Biochem.* **1986**, *152*, 6–21.
(31) Beechem, J. M. *Chem. Phys. Lipids* **1989**, *50*, 237–251.
(32) Li, N. C.; Tang, P.; Mathur, R. *J. Phys. Chem.* **1961**, *65*, 1074–1076.
(33) Eftink, M. R. In *Methods of Biochemical Analysis: Protein Structure Determination*; Suelter, C. H., Ed.; Wiley: New York, 1991; Vol. 35, pp 127–205.
(34) Gudgin, E.; Lopez-Delgado, R.; Ware, W. R. *J. Phys. Chem.* **1983**, *87*, 1559–1565.
(35) Hinman, R. L.; Whipple, E. B. *J. Am. Chem. Soc.* **1962**, *84*, 2534–2539.
(36) Hinman, R. L.; Lang, J. *J. Am. Chem. Soc.* **1964**, *86*, 3796–3806.
(37) Szabo, A. G. In *Time-Resolved Fluorescence Spectroscopy in Biochemistry and Biology*; Cundall, R. B., Dale, R. E., Eds.; Plenum Press: New York, 1983; pp 621–622.
(38) Yagil, G. *Tetrahedron* **1967**, *23*, 2855–2861.

Table II. Time-Resolved Fluorescence Data for W(1) in H_2O and D_2O at 25 °C[a]

	α_1 (350 nm)	τ_1, ns	τ_2, ns	χ_r^2
pH 5.5[b]		6.12		2.51
	0.14	3.79	6.37	1.63
pD 7.0[c]		5.72		2.23
	0.17	3.32	6.21	1.22
pH 10.5[d]		4.52		3.17
	0.20	2.88	4.78	1.24
pD 10.5[e]		7.67		3.89
	0.21	5.04	8.08	1.81

[a] 296-nm excitation wavelength. Global analysis of experiments at 5-nm intervals. [b] Data from ref 9, 320–370 nm. [c] 335–375 nm. [d] Data from ref 9, 320–395 nm. [e] 330–390 nm.

pH(D) 3.5 to 6 there is little or no deuterium isotope effect. The quantum yields in H_2O and D_2O are the same within experimental error, though the D_2O values are consistently about 4% higher. Beyond pH(D) 6 the quantum yield of W(1) in H_2O begins to drop, while it remains almost constant in D_2O. The decrease in quantum yield in H_2O and concomitant increase in deuterium isotope effect follows the titration of the amino group. The quantum yield ratio in D_2O and H_2O increases from about 1 in the zwitterion to 1.7 in the anion (Table I). The isotope effect in tryptophan zwitterion is dominated by the intramolecular proton transfer. However, in tryptophan anion it undoubtedly represents the intrinsic process that occurs in W(1) anion and other indoles.

The effect of amino group charge on the deuterium isotope effect in constrained tryptophan derivatives was investigated in a series of structural analogs of W(1) (Table I). Two analogs, THC and W(1c), that lack the amino group have large isotope effects with quantum yield ratios of about 2 at neutral pH. The analog W(1a), with an amino group in the same position as it is in W(1), shows little isotope effect until the amino group deprotonates. In another analog, W(2), the amino group is not constrained in the cyclohexene ring. The W(2) zwitterion has a modest isotope effect with a quantum yield ratio of 1.5, which increases to 1.8 in the anion. This is opposite to the intramolecular proton transfer in tryptophan, where a positive charge on the amino group increases the deuterium isotope effect.

Time-Resolved Fluorescence. Table II presents fluorescence lifetime data for W(1) at 25 °C in H_2O and D_2O obtained from global analyses of time-resolved emission spectral data. As previously reported, the data in H_2O at pH 5.5 and 10.5 were best fit by a closely spaced double exponential decay.[9] The lifetimes are 6.4 and 3.8 ns for the zwitterion and 4.8 and 2.9 ns for the anion. In D_2O at pD 7.0 and 10.5 a double exponential was also clearly the best fit. The zwitterion has lifetimes of 6.2 and 3.3 ns, very similar to the liftimes at pH 5.5, and the anion has lifetimes of 8.1 and 5.0 ns, a 1.7-fold increase over the lifetimes at pH 10.5. The biexponential decay represents the two ground-state conformers of W(1).

The deuterium isotope effect is due to a change in the rate of a nonradiative process. Table I summarizes the radiative and nonradiative rates of constrained tryptophans at 25 °C in H_2O and D_2O. The radiative rate k_r is calculated from quantum yield and lifetime data[19]

$$k_r = \Phi/\bar{\tau} \tag{1}$$

where $\bar{\tau}$ is the average lifetime

$$\bar{\tau} = \sum_i \alpha_i \tau_i / \sum_i \alpha_i \tag{2}$$

Knowing the radiative rate, the nonradiative rate k_{nr} is calculated from the average lifetime

$$\bar{\tau}^{-1} = k_r + k_{nr} \tag{3}$$

In the W(1) zwitterion, both radiative and nonradiative rates are independent of solvent isotope. However, in the W(1) anion only the radiative rate is the same in H_2O and D_2O. The nonradiative rate is 2.3-fold faster in H_2O than in D_2O. The insensitivity of the radiative rate to solvent isotope indicates that the electronic structure in the lowest excited state is not affected by the isotopic composition of the solvent. This conclusion is substantiated in the structural analogs of W(1). In the absence of a positively charged amino group the nonradiative rates of the analogs are likewise 2.4- to 2.5-fold faster in H_2O than in D_2O. The positively charged amino group depresses the isotope effect on the nonradiative rate to different extents, depending on the compound.

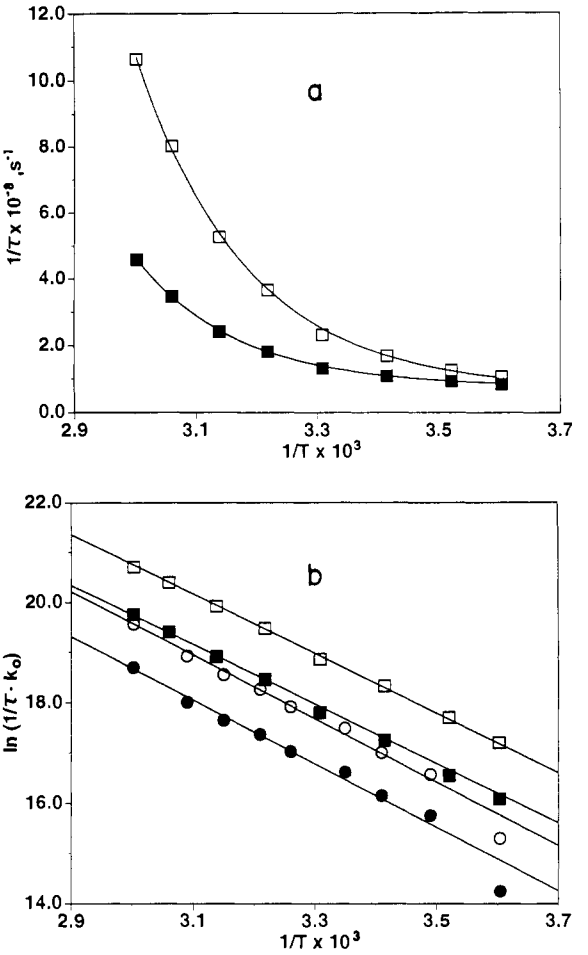

Figure 2. Temperature dependence of fluorescence lifetime of W(1) in H_2O and D_2O. Points are lifetime data from Table III. (a) Nonlinear least-squares fit to eq 4: (□) pH 11.0, (■) pD 11.0. (b) Plot of ln ($\tau^{-1} - k_0$) vs $1/T$ and line calculated from ln $A - E^*/RT$ using Arrhenius parameters from global analysis in Table IV: (○) pH 6.1, (●) pD 6.1, (□) pH 11.0, (■) pD 11.0.

Temperature Dependence of Lifetime. The isotopically sensitive nonradiative process is temperature dependent in simple indoles.[13,23,39] The temperature dependence of the fluorescence lifetime is included as an Arrhenius term in eq 3

$$\bar{\tau}^{-1} = k_0 + A \exp(-E^*/RT) \tag{4}$$

where k_0 is the total temperature-independent rate

$$k_0 = k_r + k_{nr}^0 \tag{5}$$

k_{nr}^0 is the temperature-independent nonradiative rate, A is the frequency factor, E^* is the activation energy, R is the gas constant, and T is absolute temperature. The fluorescence decay of W(1) zwitterion and anion was measured at 350-nm emission wavelength in H_2O and D_2O in the temperature range 4–60 °C. Experiments were also done on *N*-methylindole for comparison with the literature. Arrhenius parameters were determined by the usual two-step procedure of fitting the decay curves at each temperature to single- and double-exponential functions (Table III) followed by a nonlinear fit of the resulting lifetimes or average lifetimes to eq 4. Figure 2a shows the nonlinear fits of the data for W(1)

(39) Walker, M. S.; Bednar, T. W.; Lumry, R. In *Molecular Luminescence*; Lim, E. C., Ed.; Benjamin: New York, 1969; pp 135–152.

Table III. Temperature Dependence of Fluorescence Lifetime in H_2O and D_2O[a]

	W(1)				*N*-methylindole	
	τ, ns		$\bar{\tau}$, ns		τ, ns	
t, °C	pH 6.1	pD 6.1	pH 11.0	pD 11.0	H_2O	D_2O
4.3	7.46	7.62				9.53
4.4			9.22	11.3		
8.1					9.26	
10.9			7.85	10.6		
13.5	6.88	7.32			8.99	9.27
19.7	6.49	7.14	5.89	9.10		9.08
20.7					8.58	
25.7	5.91	6.84				8.79
28.7					7.68	
29.1			4.27	7.53		
33.3	5.26	6.47				8.38
34.9					6.88	
37.6			2.72	5.47		
38.5	4.63	6.07				7.88
39.5					6.26	
44.0	4.08	5.69				7.43
45.5			1.90	4.12		
45.9					5.30	
50.3	3.38	5.10				6.69
52.0					4.31	
53.6			1.25	2.88		
60.0	2.24	3.82	0.94	2.18	3.24	5.34

[a] χ_r^2 values averaged about 1.6, 4, and 1.8 for single-exponential fits for W(1) at pH(D) 6.1, W(1) at pH(D) 11.0, and *N*-methylindole and about 1.8 for double exponential fits for W(1) at pH(D) 11.0.

anion in H_2O and D_2O. Parameters were also determined in one step by fitting the decay curves directly to an Arrhenius function

$$I(t) = \alpha \exp[-t(k_0 + Ae^{-E^*/RT})] \quad (6)$$

in single-curve analyses of the data at each temperature or global analyses of the data at different temperatures.[31] In the global analyses the data sets for H_2O and D_2O were analyzed simultaneously with the temperature-independent rate k_0 and activation energy E^* assumed to be independent of solvent isotope. Figure 2b plots ln $(\tau^{-1} - k_0)$ vs $1/T$ together with calculated lines using the Arrhenius parameters from the global analyses for W(1) zwitterion and anion. Table IV summarizes the Arrhenius parameters obtained by various methods.[40] The results from one-step single-curve analyses at different temperatures are given as average values. The k_0 values obtained from nonlinear fits of lifetime data to eq 4 and from single-curve analyses according to eq 6 are almost identical in H_2O and D_2O for W(1) zwitterion and *N*-methylindole and within the error for W(1) anion, indicating that the temperature-independent rate k_{nr}^0 is insensitive to solvent isotope. The activation energy E^* also appears to be the same in H_2O and D_2O. Literature values for *N*-methylindole[39] and indole[23] support these conclusions. For equal activation energies, the frequency factors A are larger in H_2O than in D_2O by 2- to 3-fold. Perusal of the numbers in Table IV reveals why the deuterium isotope effect is absent in the W(1) zwitterion but present in the anion at 25 °C. In both the nonlinear and global fits the temperature-independent rate k_0 is almost twice as fast in the zwitterion as in the anion, tending to swamp out the isotope effects on the temperature-dependent nonradiative rate of the zwitterion. (The value of k_0 is poorly determined in the single-curve analyses for the anion, presumably because a single exponential term is assumed in eq 6.) The larger k_0 value in the zwitterion is mostly due to the temperature-independent nonradiative rate k_{nr}^0, which is at least 2-fold faster in the zwitterion than in the anion. The temperature-dependent nonradiative rate $k_{si} = A \exp(-E^*/RT)$, which is sensitive to solvent isotope through the frequency factor, is faster in the anion than in the zwitterion. Thus, two opposing phenomena, smaller k_{nr}^0 and larger k_{si} values, combine to make the isotopically sensitive rate more competitive in the W(1) anion.

(40) The Arrhenius parameters for W(1) zwitterion differ from the values reported in refs 8 and 9 because of erroneous cell temperatures. Analysis of the data for W(1) at pH 7.0 in Table IV of ref 8 with correct temperatures gives $A = 4.8 \times 10^{12}$ s^{-1}, $E^* = 6.6$ kcal/mol for the linear fit assuming $k_0 = 9.9 \times 10^7$ s^{-1}; and $A = 6.4 \times 10^{15}$ s^{-1}, $E^* = 11.2$ kcal/mol for the linear fit assuming $k_0 = 1.25 \times 10^8$ s^{-1}.

Scheme I

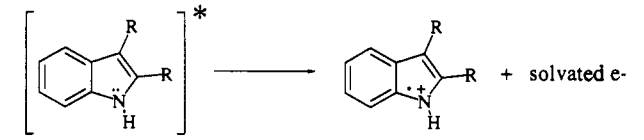

Scheme II

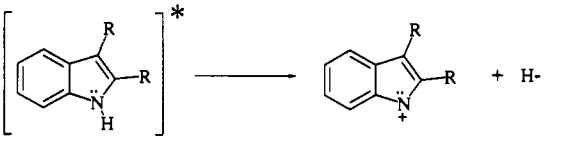

Scheme III

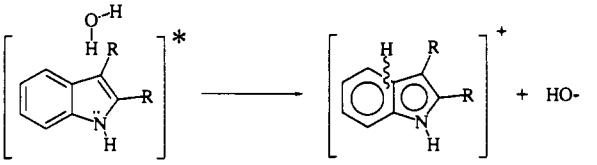

Scheme IV

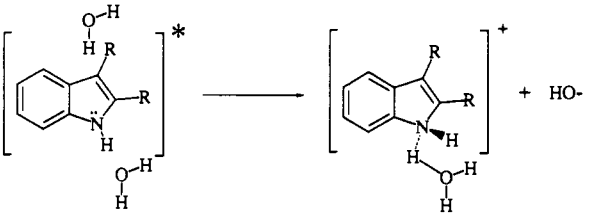

Scheme V

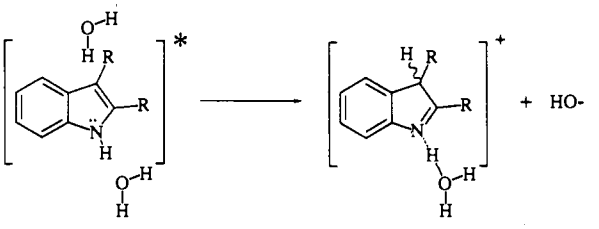

Conclusions

The environmental sensitivity of tryptophan fluorescence derives in part from the multiple nonradiative decay processes possible for the indole chromophore. Nonradiative channels known or proposed for the decay of the lowest excited singlet state of tryptophan and other indoles are internal conversion, intersystem crossing, photoionization, and excited-state proton and electron transfer reactions. Depending on the particular system, the nonradiative rate k_{nr} usually contains contributions from several pathways. The individual rates are generally unknown. The fluorescence quantum yield and lifetime will have a deuterium isotope effect if the isotopically sensitive rates are competitive with the radiative and other nonradiative rates. For example, tryptophan ethyl ester has a quantum yield ratio in H_2O to D_2O of 1.1[13] and shows no photochemical H–D exchange at C4 of indole.[9] The average fluorescence lifetime of tryptophan ethyl ester is only 0.5 ns,[6] suggesting that an isotopically insensitive rate, presumably electron transfer, is much faster than the proton transfer rate. W(1) zwitterion and *N*-methylindole[12,41] have quantum yield ratios in H_2O to D_2O of 1.05–1.09 and lifetimes of 6–10 ns at room temperature. The temperature-independent radiative and non-

(41) Yu, H-T.; Colucci, W. J.; McLaughlin, M. L.; Barkley, M. D. *J. Am. Chem. Soc.*, following paper in this issue.

Table IV. Arrhenius Parameters in H_2O and D_2O

analysis	10^{-7} k_0, s^{-1}	A, s^{-1}	E^*, kcal/mol	10^{-7} k^0_{nr}, s^{-1}	10^{-7} k_{si},[b] s^{-1}
		W(1), pH 6.1			
nonlinear fit	12.6	8.6×10^{15}	11.4	5.3	3.9
single curve	12.4 ± 0.3	$(9.5 \pm 0.6) \times 10^{15}$	11.43 ± 0.01	5.1	3.9
global	13.0	5.9×10^{16}	12.6	5.7	3.4
		W(1), pD 6.1			
nonlinear fit	12.8	1.7×10^{15}	10.9	4.8	1.7
single curve	12.5 ± 0.2	$(4 \pm 1) \times 10^{15}$	11.41 ± 0.03	4.5	1.5
global	13.0	2.4×10^{16}	12.6	5.0	1.4
		W(1), pH 11.0			
nonlinear fit	6.9	1.6×10^{16}	11.0	1.0	14.1
single curve	23 ± 21	$(1.8 \pm 0.2) \times 10^{16}$	11.3 ± 0.1	17	9.3
global	7.9	5.3×10^{16}	11.8	2.0	12.7
		W(1), pD 11.0			
nonlinear fit	7.7	2.1×10^{16}	11.8	1.8	4.7
single curve	11 ± 4	$(8 \pm 2) \times 10^{15}$	11.4 ± 0.2	5	3.5
global	7.9	2.0×10^{16}	11.8	2.0	4.6
		N-Methylindole, H_2O			
nonlinear fit	10.4	2.3×10^{17}	13.8	4.7[c]	1.8
single curve	10 ± 4	$(2.10 \pm 0.05) \times 10^{16}$	12.1 ± 0.4	4[c]	2.8
global	10.3	7.9×10^{16}	13.1	4.6[c]	2.0
ref 39	10.6	6.2×10^{16}	13.1	3.3	1.5
		N-Methylindole, D_2O			
nonlinear fit	10.3	9.2×10^{15}	12.3	4.6[c]	0.96
single curve	10 ± 2	$(1.2 \pm 0.8) \times 10^{16}$	12.0 ± 0.6	4[c]	1.9
global	10.3	3.3×10^{16}	13.1	4.6[c]	0.85
ref 39	10.7	1.7×10^{15}	11.2	3.5	1.0
		Indole, H_2O			
ref 39	13.9	2.1×10^{14}	8.5	2.9	12.2
ref 23	15.3	9.3×10^{15}	10.8	7.0	11.1
		Indole, D_2O			
ref 39	14.0	1.7×10^{15}	10.4	3.0	4.0
ref 23	14.2	2.9×10^{15}	10.8	6.0	3.5

[a] χ_r^2 values averaged about 1.6, 3.5, and 1.6 for single-curve fits to eq 6 and were 2.6, 4.8, and 1.9 for global fits for W(1) at pH(D) 6.1, W(1) at pH(D) 11.0, and *N*-methylindole, respectively. [b] $k_{si} = A \exp[-E^*/RT]$ at 25 °C. [c] k_r value taken from ref 41.

Scheme VI

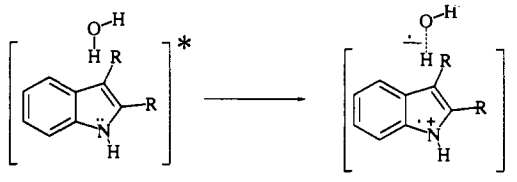

radiative rates are fast compared to the isotopically sensitive rate at this temperature. The intrinsic isotope effect is an important temperature-dependent nonradiative decay pathway for indoles in water.

We can conceive of at least six mechanisms for the isotopically sensitive temperature-dependent quenching process in W(1) and other indoles: (1) photoionization to yield a radical cation and a solvated electron (Scheme I), (2) hydride transfer from the indole nitrogen to solvent leading to a resonant nitrenium ion (Scheme II), (3) proton transfer from solvent to a basic site on the ring (Scheme III), (4) solvent-mediated N–H exchange leading to partial charge build up on the indole nitrogen (Scheme IV), (5) solvent-mediated tautomerizations resulting in N–H abstraction (Scheme V), and (6) electron transfer to solvent forming an exciplex (Scheme VI).

A deuterium isotope effect occurs in all indoles in water. Although intramolecular proton transfer appears to rationalize much of the isotope effect in tryptamine and tryptophan,[20,21] another isotopically sensitive process is clearly present.[42,43] In simple indoles the isotope effect argues more strongly for proton or hydride transfers, but an isotope effect is conceivable for N–H exchange and tautomerization as well. Photoionization has also been invoked to explain the intrinsic isotope effect.[13,22] For photoionization to depend on solvent isotope, however, electron ejection from excited indole would have to be coupled to solvent.[23] The stopped-flow absorbance and fluorescence experiments of Nakanishi and co-workers[42-44] indicate that the isotope effect derives from solvent protons rather than from the indole N–H proton. The observation of an isotope effect in *N*-methylindole supports this conclusion.[39] The N–H structural feature, while favored, is not required for the intrinsic isotope effect.

Most indoles have a constant quantum yield and isotope effect over a notably broad pH range.[14,16,17,45] This argues for pH-independent quenching mechanisms catalyzed by water alone, such as photoionization and electron transfer, and against acid–base mechanisms such as hydride transfer, proton transfer, and to a lesser extent N–H exchange or tautomerizations, both of which are push–pull-type mechanisms that are overall neutral reactions. In the ground state, N–H exchange is moderately pH sensitive, increasing only 10-fold for 2 pH units on either side of the minimum at pH 4.5.[44] The effect of pH on tautomerizations can be inferred from the rate of ground-state exchange at C3, which is significant only below pH 5.[46] In either case the exchange rate would have to be 10^6-10^8 times faster in the excited state to compete with fluorescence emission. Excited-state proton transfer and tautomerizations of aromatic protons can be detected by photochemical isotope exchange.[10] As described in the companion paper, we see no H–D exchange in 2-methylindole at neutral pH.[41] Therefore, if the quenching mechanism involves proton transfer,

(42) Nakanishi, M.; Tsuboi, M. *Chem. Phys. Lett.* **1978**, *57*, 262–264.
(43) Nakanishi, M.; Kobayashi, M.; Tsuboi, M.; Takasaki, C.; Tamiya, N. *Biochemistry* **1980**, *19*, 3204–3208.
(44) Nakanishi, M.; Nakamura, H.; Hirakawa, A. Y.; Tsuboi, M.; Nagamura, T.; Saijo, Y. *J. Am. Chem. Soc.* **1978**, *100*, 272–276.
(45) Feitelson, J. *Isr. J. Chem.* **1970**, *8*, 241–252.
(46) Challis, B. C.; Millar, E. M. *J. Chem. Soc., Perkin Trans. II* **1972**, 1618–1624.

either the proton transfer occurs at "invisible" sites such as ring junctions and the indole nitrogen or the transfer is only partial, effectively formation or tightening of a hydrogen bond.[47]

The quantum yield and lifetime of indoles are highly temperature dependent. Table IV summarizes the Arrhenius data for several indoles in H_2O and D_2O. W(1) zwitterion and anion, *N*-methylindole, and indole have frequency factors A of 10^{15}–10^{17} s^{-1} and activation energies E^* of 11–13 kcal/mol. Such values are suggestive of electronic rather than nuclear motions.[48] For mechanisms involving substantial bond breaking and bond forming to hydrogen, an isotope effect on A and perhaps also E^* is expected. This is, in fact, the case for tryptophan zwitterion,[13] which has two isotopically sensitive quenching mechanisms. Eisinger and Navon[12] and Robbins et al.[22] noted considerable curvature in the Arrhenius plot for tryptophan, suggestive of its composite nature. In W(1) zwitterion and anion as well as in *N*-methylindole and indole the activation energy is independent of solvent isotope. Hence it is the frequency of the intrinsic quenching process that is isotope dependent.

Previously, the temperature-dependent nonradiative process in indoles was thought to be photoionization.[13,22] However, picosecond laser photolysis studies of indole and tryptophan in water show that electron ejection and solvation occur prior to formation of the relaxed singlet excited state.[49] This result rules out photoionization as a pathway for deactivation of the lowest excited single state. Photoionization from a prefluorescent state does not affect the fluorescence lifetime but lowers the apparent fluorescence quantum yield (and apparent radiative rate calculated from eq 1).[50] Lee and Robinson[23,51] invoked electron transfer from the solvent-relaxed excited state to a water cluster to explain the intrinsic quenching process in indole. They suggest that a cooperative change in noncovalent hydrogen bonding due to electron solvation within this cluster accounts for the large activation energy. The isotope effect on the frequency factor is attributed to a Franck–Condon effect associated with ionization. However, the small deuterium isotope effects on the rates of electron hydration in water, which show k_H/k_D of only 1.1–1.2, do not support this explanation.[52] Electron transfer to σ^* of an H(D)–O bond in an exciplex, as illustrated in Scheme VI, is more likely to exhibit 2- to 3-fold isotope effects on A (Table IV). This charge-transfer exciplex is analogous to the first step in the trapping of solvated electrons to form $H(D)_2$. The formation of $H(D)_2$ from solvated electrons in 1:1 H_2O/D_2O has a k_H/k_D of 4.7 and occurs on the nanosecond time scale.[53-55] Finally, we need to consider the overall fate of the indole radical cation–water radical anion pair formed after electron transfer. Back reaction to a vibrationally excited ground state is probably a major pathway as already noted by others considering photoionization.[51,56,57] The water radical anion could transfer a hydrogen atom to the indole radical cation, yielding protonated indole and hydroxide ion with or without H–D exchange. Hydrogen atom transfer to solvent is another possibility, leading to a nitrenium species that could give oxidized products.[1]

In summary, two plausible mechanisms for the intrinsic quenching process of indoles in water are consistent with the pH dependence and temperature dependence of the deuterium isotope effect: "invisible" or incomplete proton transfer and exciplex formation. The following paper examines excited-state proton transfer reactions in simple indoles.[41]

Acknowledgment. We thank Professor Richard D. Gandour for helpful discussions. This work was supported by NIH Grant GM42101.

Registry No. W, 73-22-3; W(1), 42438-90-4; W(1a), 16502-01-5; W(1c), 143121-58-8; W(2), 51145-64-3; THC, 942-01-8; *N*-methylindole, 603-76-9.

(47) Gandour, R. D.; Nabulsi, N. A. R.; Fronczek, F. R. *J. Am. Chem. Soc.* **1990**, *112*, 7816–7817.
(48) Kavarnos, G. J. *Top. Curr. Chem.* **1990**, *156*, 21–58.
(49) Mialocq, J. C.; Amouyal, E.; Bernas, A.; Grand, D. *J. Phys. Chem.* **1982**, *86*, 3173–3177.
(50) Birks, J. B. National Bureau of Standards Special Publication 466; *Standardization in Spectrophotometry and Luminescence Measurements*; U.S. Government Printing Office: Washington, DC, 1977; pp 1–11.
(51) Lee, J.; Robinson, G. W. *J. Chem. Phys.* **1984**, *81*, 1203–1208.
(52) Gauduel, Y.; Pommeret, S.; Migus, A.; Antonetti, A. *J. Phys. Chem.* **1991**, *95*, 533–539.
(53) Anbar, M.; Meyerstein, D. *Trans. Faraday Soc.* **1966**, *62*, 2121–2131.
(54) Anbar, M.; Meyerstein, D. *J. Chem. Soc., Chem. Commun.* **1966**, 57–58.
(55) Anbar, M.; Meyerstein, D. In *Radiation Chemistry of Aqueous Systems*; Stein, G., Ed.; Weizmann Science Press: Jerusalem, 1968; pp 109–155.
(56) Baugher, J. F.; Grossweiner, L. I. *J. Phys. Chem.* **1977**, *81*, 1349–1354.
(57) Klein, R.; Tattischeff, L.; Bazin, M.; Santas, R. *J. Phys. Chem.* **1981**, *85*, 670–677.